PHILOSOPHICAL TRANSACTIONS OF THE ROYAL SOCIETY A
MATHEMATICAL, PHYSICAL & ENGINEERING SCIENCES

Numerical Simulation of Subduction Zone Pressure-Temperature-Time Paths: Constraints on Fluid Production and Arc Magmatism

Simon M. Peacock

Phil. Trans. R. Soc. Lond. A 1991 **335**, 341-353
doi: 10.1098/rsta.1991.0050

Numerical simulation of subduction zone pressure–temperature–time paths: constraints on fluid production and arc magmatism

By Simon M. Peacock

Department of Geology, Arizona State University, Tempe, Arizona 85287-1404, U.S.A.

The location and sequence of metamorphic devolatilization and partial melting reactions in subduction zones may be constrained by integrating fluid and rock pressure–temperature–time (P–T–t) paths predicted by numerical heat-transfer models with phase diagrams constructed for metasedimentary, metabasaltic, and ultramafic bulk compositions. Numerical experiments conducted using a two-dimensional heat transfer model demonstrate that the primary controls on subduction zone P–T–t paths are: (1) the initial thermal structure; (2) the amount of previously subducted lithosphere; (3) the location of the rock in the subduction zone; and (4) the vigour of mantle wedge convection induced by the subducting slab. Typical vertical fluid fluxes out of the subducting slab range from less than 0.1 to 1 (kg fluid) m^{-2} a^{-1} for a convergence rate of 3 cm a^{-1}. Partial melting of the subducting, amphibole-bearing oceanic crust is predicted to only occur during the early stages of subduction initiated in young (less than 50 Ma) oceanic lithosphere. In contrast, partial melting of the overlying mantle wedge occurs in many subduction zone experiments as a result of the infiltration of fluids derived from slab devolatilization reactions. Partial melting in the mantle wedge may occur by a two-stage process in which amphibole is first formed by H_2O infiltration and subsequently destroyed as the rock is dragged downward across the fluid-absent 'hornblende-out' partial melting reaction.

1. Introduction

Large-scale mixing of crustal and mantle materials occurs at subduction zones where oceanic lithosphere, capped by variably hydrated oceanic crust and sediments, descends beneath either oceanic or continental lithosphere. Over time, most of Earth's continental crust has been extracted from the mantle at subduction zones. The location of volcanoes above subducting slabs, as defined by inclined seismic planes, requires that partial melting occurs in subduction zones despite the cooling effect of subducting lithosphere. Much research has focused on constraining the source region of arc magmas by petrological and geochemical investigations of the products of arc magmatism (Gill 1981); such investigations may be considered analogous to inverse methods used in geophysics. In this paper, I use a forward method to investigate zone processes based on a two-dimensional numerical model of heat transfer and metamorphic reactions. Ultimately, the complementary nature of forward and inverse methods should result in a quantitative understanding of subduction zones and arc magmatism.

Phil. Trans. R. Soc. Lond. A (1991) **335**, 341–353 341
Printed in Great Britain [115]

Numerical simulations of heat and mass transfer in subduction zones provide important constraints on processes occurring at depths greater than 50 km from which geologic samples are extremely rare. Numerous thermal models of subduction zones have been presented in the literature (Hasebe *et al.* 1970; Minear & Toksoz 1970; Oxburgh & Turcotte 1970; Toksoz *et al.* 1971; Andrews & Sleep 1974; Honda & Uyeda 1983; van der Beukel & Wortel 1986). Thermal models have been combined with petrologic models of the subducting slab and mantle wedge by Oxburgh & Turcotte (1976), Anderson *et al.* (1976, 1978, 1980), Delany & Helgeson (1978), Wyllie & Sekine (1982), and Wyllie (1988), among others.

In contrast to previous subduction zone models, the models presented in this paper specifically predict pressure–temperature–time (P–T–t) paths followed by rocks in the subducting slab and the overlying mantle wedge. Subduction zone P–T–t paths represent the P–T conditions encountered by rocks moving through an evolving (non-steady-state) thermal structure. Because of the material flow in subduction zones and the time-dependent thermal structure, subduction zone processes may be best understood by considering subducting slab and mantle wedge P–T–t paths. Subduction zone P–T–t paths can be combined with appropriate phase diagrams in order to constrain the sequence and location of metamorphic and melting reactions in the subducting slab. Of particular importance are reactions involving low-viscosity (aqueous) fluids that may trigger partial melting reactions in the overlying mantle wedge. Calculated mantle wedge P–T–t paths constrain the location of hydration, dehydration, and partial melting reactions in the sub-arc lithosphere and asthenosphere.

Recent estimates of subduction zone volatile budgets (Peacock 1990*a*) suggest that an order of magnitude more H_2O and CO_2 is subducted than can be accounted for in arc magmas. The release and ultimate fate of these volatiles may have a profound effect on the thermal, petrological, and rheological evolution of subduction zone. The results of the numerical simulations presented in this paper permit us to consider possible P–T paths followed by released volatiles and therefore place constraints on fluid processes in subduction zones.

2. Description of the numerical model

Numerical simulations of heat and mass transfer in subduction zones were conducted by using a two-dimensional finite difference model (figure 1). This model is similar to the finite difference models described in Peacock (1987*b*, 1990*b*), except that (1) oceanic geotherms were defined by calculating the conductive cooling of a mantle adiabat and (2) an analytical solution describing induced convection was incorporated into the mantle wedge. Briefly, the two-dimensional model simulates heat transfer in a subduction zone with a 26.6° dip. A spatial resolution of 1 km is used in the region of the subduction thrust to carefully monitor metamorphic reactions; elsewhere the spatial resolution is 5 km. The advective/conductive heat transfer equation was solved in two dimensions by using an explicit finite difference method. A more detailed description of the numerical method may be found in Peacock (1987*b*, 1990*b*).

Oceanic geotherms as a function of age were constructed by numerically calculating the conductive cooling of a zero-age adiabat (Jeanloz & Morris 1986). The zero-age adiabat was defined by a surface temperature of 1275 °C, a 3 °C km^{-1} adiabatic gradient in the upper 35 km (appropriate for mantle with 5–30 % partial melt), and

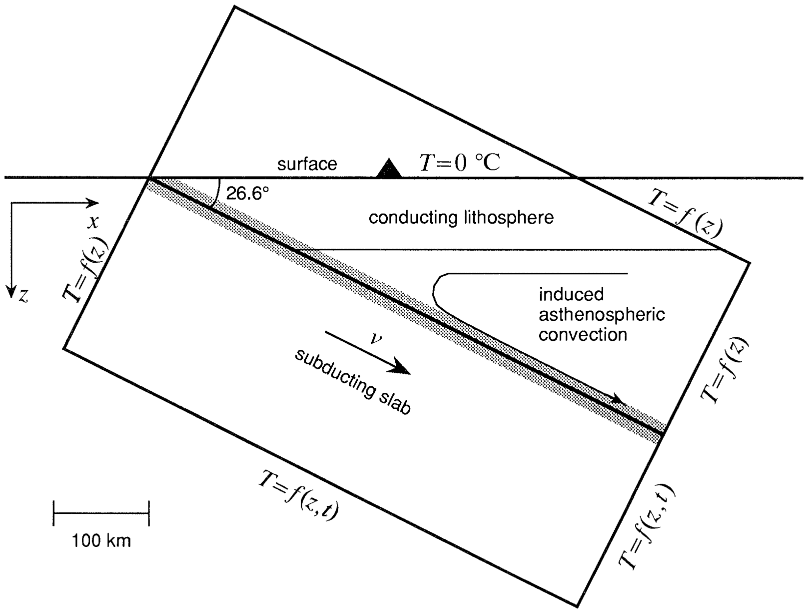

Figure 1. Geometry and boundary conditions used in the numerical model of subduction zone heat transfer. The two-dimensional 400×600 km grid is oriented at a 26.6° angle to the Earth's surface, such that the subduction thrust is parallel to one of the model axes. To carefully monitor reactions in the subducting oceanic crust, a 1 km finite-difference grid spacing is used within 10 km of the subduction thrust (stippled region); elsewhere the grid spacing is 5 km. Rocks in the subducting slab move downward, parallel to the subduction thrust at a constant velocity. Rocks in the overlying asthenosphere move along steady-state streamlines defined by Batchelor's (1967) analytical solution for two-dimensional fluid flow in a corner. The surface temperature is kept constant at 0 °C. Boundaries labelled $T = f(z)$ are kept at a constant temperature defined by the initial oceanic geotherm. Boundaries labelled $T = f(z, t)$ are reset during the advection time step and held constant during the conduction time step.

a 0.3 °C km^{-1} adiabatic gradient below 35 km (Stacey 1977; Basaltic Volcanism Study Project 1981; Jeanloz & Morris 1986). During cooling, the surface temperature was fixed at 0 °C and the thermal diffusivity at 10^{-6} m^2 s^{-1}. The calculated oceanic geotherms agree well with oceanic heat flow measurements for $t < 80$ Ma; for older oceanic lithosphere, the conductive cooling model predicts slightly lower heat flow values than are observed.

Induced flow in the asthenospheric wedge overlying the subducting slab (figure 1) was simulated using an analytical solution for two-dimensional incompressible fluid flow in a corner (Batchelor 1967, pp. 224–227). The fluid is assumed to have a uniform viscosity throughout the wedge. A no-slip boundary condition is used at the base of the conducting lithosphere (defined as the 1300 °C isotherm) and a constant slip equal to the slab velocity is used at the top of the subducting slab. More complex induced flow models could be constructed, but this steady-state model represents an end-member model that may be compared with simulations run with no induced convection.

A series of numerical experiments were conducted in order to determine the primary variables that control rock *P–T–t* paths in subduction zones. Each numerical experiment simulated up to 100 Ma of thermal evolution. The following

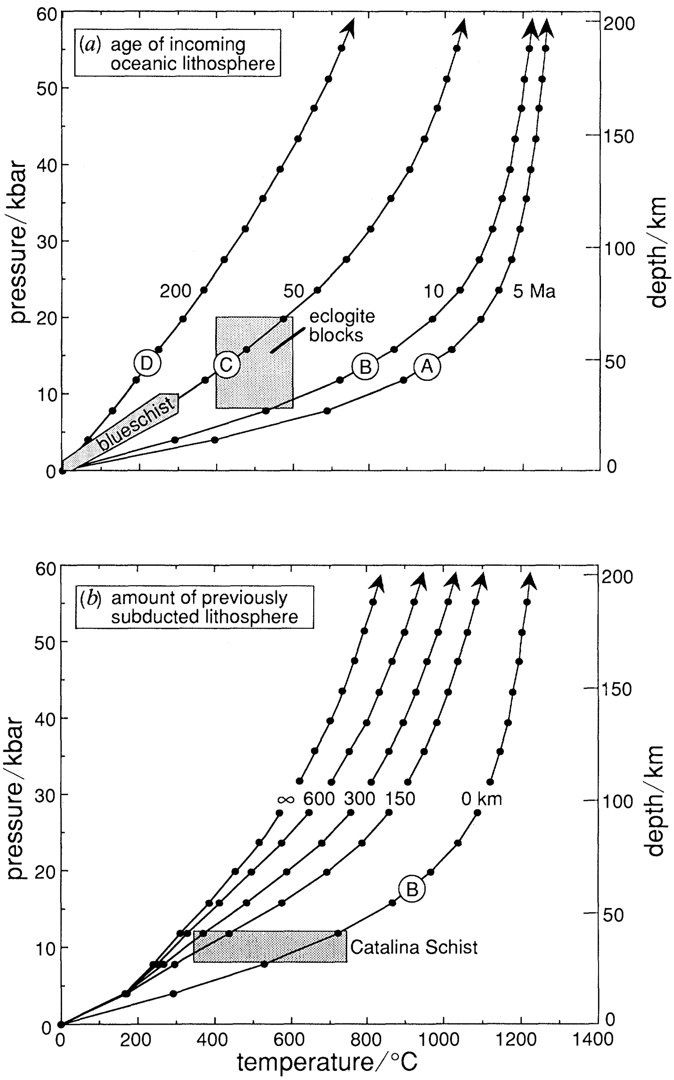

Figure 2. Subduction zone P–T–t paths predicted by the two-dimensional, heat-transfer model and selected pressure–temperature constraints based on investigations of ancient subduction zones. Solid circles represent intervals of 1 Ma; open circles represent intervals of 10 Ma. Selected P–T–t paths are labelled with letters for use in later figures. (*a*) Calculated P–T–t paths for the top of the subducted oceanic crust as a function of the age of the incoming oceanic lithosphere. Convergence rate is 3 cm a^{-1}. Prograde blueschist P–T paths (Ernst 1988) and P–T conditions recorded by eclogite blocks (Evans & Brown 1986) shown by stippled regions. (*b*) P–T–t paths followed by the top of the subducting oceanic crust as a function of the amount of previously subducted lithosphere (convergence rate × time). Convergence rate is 3 cm a^{-1}. The curve labelled '∞' represents the steady-state P–T–t path. The predicted cooling with time is consistent with the P–T conditions preserved in the Catalina Schist inverted metamorphic gradient (Platt 1975; Sorensen 1986, 1988). (*c*) P–T–t paths as a function of position (subducting oceanic crust, mantle wedge) in the subduction zone. Convergence rate is 3 cm a^{-1}. Downward conduction of heat into the subducting slab results in warmer P–T–t paths for the top of the subducting oceanic crust as compared with the base. Mantle wedge material, located 5 km from the top of the subducting slab, that is not dragged down with the subducting slab will follow isobaric cooling P–T–t paths. P–T–t path G represents the approximate path followed by mantle material that is dragged down by the

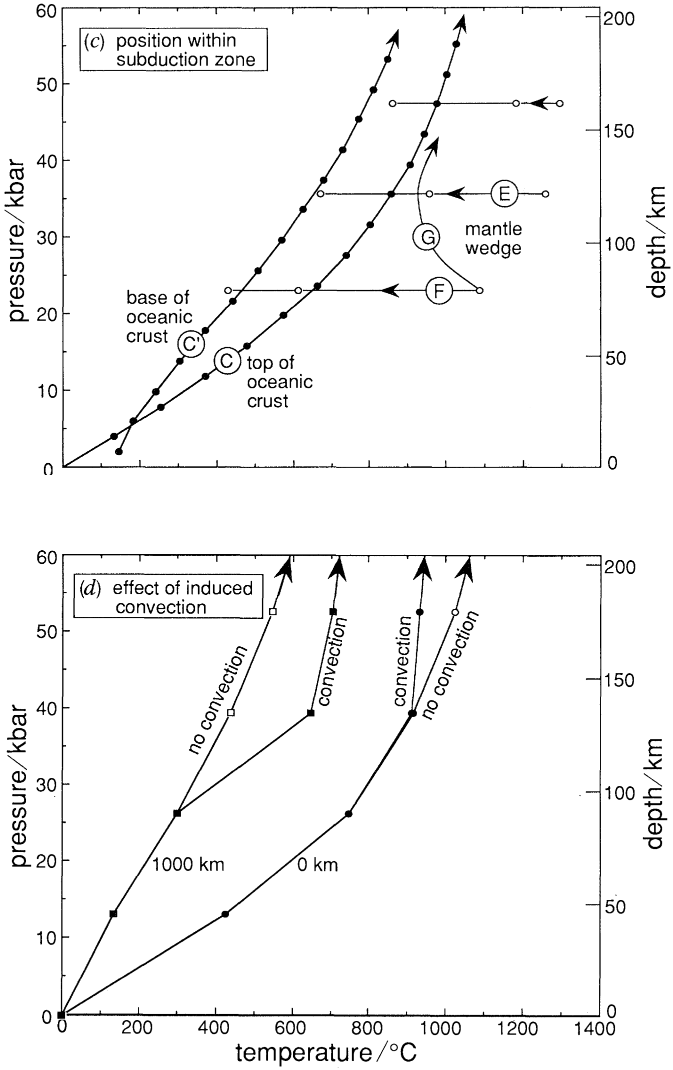

subducting slab. (*d*) *P–T–t* paths followed by the top of the subducting slab as a function of the vigour of induced convection and the amount of previously subducted material. Convergence rate is 10 cm a^{-1}. Initially, induced mantle wedge convection results in slightly cooler slab *P–T–t* paths. As subduction progresses, slab *P–T–t* paths remain warm because of induced mantle wedge convection.

parameters were varied during individual numerical experiments: (1) the initial age of the oceanic lithosphere; (2) the convergence rate; (3) the nature of metamorphic dehydration reactions; (4) the amount of shear heating; and (5) the presence of induced mantle convection. Each numerical experiment produces a data set containing the thermal structure of the subduction zone as a function of time from which *P–T–t* paths were calculated for selected rocks in the subducting slab and the mantle wedge.

3. Results

The results of the numerical experiments demonstrate that the primary factors controlling rock P–T–t paths are: (1) the initial thermal structure; (2) the amount of previously subducted lithosphere (convergence rate × time); (3) the position of the rock in the subduction zone; and (4) and the vigour of induced mantle convection.

The initial thermal structure is the dominant factor in determining the P–T–t path followed by the earliest subducted oceanic crust (figure 2*a*). Subduction zones that form in young, relatively hot, oceanic lithosphere result in warmer slab P–T–t paths as compared with subduction zones that form in older oceanic lithosphere. Subduction zones initiated in 5–10 Ma oceanic lithosphere result in slab P–T–t paths that exceed 1100 °C at 30 kbar†. In contrast, subduction zones formed in 200 Ma oceanic lithosphere result in slab P–T–t paths passing through *ca*. 500 °C at 30 kbar. Blueschist P–T paths and the P–T conditions of eclogites are consistent with P–T–t paths calculated for *ca*. 50 Ma oceanic lithosphere (figure 2*a*).

The amount of previously subducted lithosphere (convergence rate × time) is a major factor in controlling subduction zone P–T–t paths (figure 2*b*). The advection of heat by the subducting slab dominates the thermal structure of subduction zones. As more lithosphere is subducted, subducting oceanic crust P–T–t paths follow cooler trajectories. For a subduction zone formed in 10 Ma oceanic crust, the initial subducting oceanic crust P–T–t path intersects *ca*. 1100 °C at 30 kbar; P–T–t paths for oceanic crust subducted after 600 km of previous subduction intersects *ca*. 700 °C at 30 kbar. The predicted cooling with time is consistent with inverted metamorphic gradients preserved in palaeosubduction zones such as the Catalina Schist and Pelona Schist of southern California (Peacock 1987*b*). Qualitatively, P–T–t paths calculated for mature subduction zones resemble P–T–t paths calculated for subduction zones formed in older oceanic lithosphere. Cool, approximately steady-state conditions are achieved after 50–100 Ma of subduction.

Rocks in the subducting slab and the overlying mantle wedge follow strikingly different P–T–t paths (figure 2*c*). Subducting oceanic crust follows P–T–t paths characterized by increasing pressure and temperature. Conduction of heat downward from the overlying mantle wedge into the top of the subducting slab results in warmer P–T–t paths for the top of the oceanic crust as compared to the base (figure 2*c*). In the absence of mantle wedge convection induced by the subducting slab, mantle wedge rocks follow isobaric cooling P–T–t paths (figure 2*c*). In subduction zones with induced mantle convection, rocks in the mantle wedge near the subducting slab first cool approximately isobarically, and subsequently undergo compression with minor heating as they are dragged downward by the slab (figure 2*c*).

In addition to strongly influencing mantle wedge P–T–t paths, induced convection also affects subducting slab P–T–t paths (figure 2*d*). Slab P–T–t paths calculated with and without induced mantle wedge convection diverge at the base of the overriding lithosphere (100 km in figure 2*d*). Initially, induced convection results in slightly cooler slab P–T–t paths because the dragging down of cool mantle wedge material next to the slab results in reduced thermal gradients in the subduction thrust region and therefore reduced downward conduction. With continued subduction, induced convection results in substantially warmer slab P–T–t paths, as

† 1 bar = 10^5 Pa.

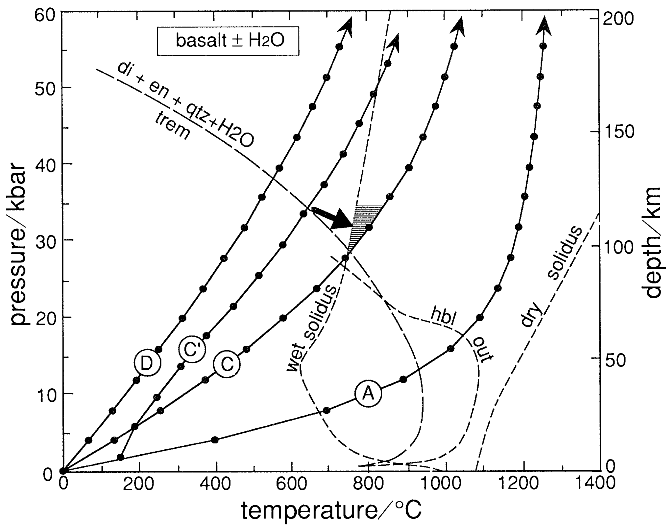

Figure 3. *P–T–t* paths (solid lines) and experimental melting relations (short dashed lines) for the hydrous basalt system. The addition of excess H_2O drastically decreases the melting temperature of basalt (dry solidus: Green 1982; wet solidus: Lambert & Wyllie 1972). The 'hbl out' curve represents fluid-absent partial melting of hornblende-bearing metabasalt (Green 1982). Long-dashed line represents calculated tremolite dehydration reaction using the thermodynamic data of Berman (1988). Subducted oceanic crust following *P–T–t* paths cooler than path C will dehydrate before reaching melting reactions, suggesting that arc magmas in cool subduction zones are not derived from partial melting of the oceanic crust. Warmer *P–T–t* paths predicted for subduction zones developed in young oceanic lithosphere result in substantial partial melting associated with the breakdown of hornblende at pressures less than *ca.* 28 kbar. If the top (path C) and base (path C′) of the subducting oceanic crust straddle the wet solidus at *ca.* 30 kbar, then fluids released by dehydration reactions (arrow) could trigger partial melting in overlying oceanic crust (striped region).

compared with experiments with no convection, because the overlying mantle wedge is replenished with hot asthenosphere. The overall effect of induced mantle wedge convection on slab *P–T–t* paths is to retard the rapid cooling effect of subducting lithosphere shown in figure 2*b*.

Additional processes, such as shear heating (frictional heating, viscous dissipation), metamorphic reactions, and metamorphic fluid flow affect subduction zone *P–T–t* paths, but only to a minor extent. The thermal effect of shear heating is proportional to the shear stress and convergence rate of the subduction zone. As compared with numerical experiments with no shear heating, numerical experiments that incorporate shear heating (maximum shear stress is 250 bar, $v = 3$ cm a^{-1}) result in subducting slab *P–T–t* paths that are only *ca.* 50 °C warmer. Numerical experiments that incorporate prograde metamorphic reactions that consume 50 kJ kg^{-1} result in subducting slab *P–T–t* paths that are only 5 °C cooler (Peacock 1990*b*). The thermal effect of metamorphic fluid flow in subduction zones has been discussed in earlier papers (Peacock 1987*c*, 1990*b*). The results of these previous experiments suggest a maximum effect of fluid flow of *ca.* 100 °C on mantle wedge *P–T–t* paths if all fluids released by devolatilization reactions in the subducting oceanic crust flow upward into widely spaced (more than 10 km) channels in the mantle wedge. Other flow geometries, such as pervasive upward fluid flow or slab-parallel fluid flow, result in a negligible effect on mantle wedge and subducting slab P–T–t paths.

4. Discussion

(a) *Dehydration and partial melting of the subducting slab*

Calculated subduction slab P–T–t paths can be combined with a phase diagram for hydrous basalt (figure 3) to predict the sequence of metamorphic and igneous reactions encountered by the subducting oceanic crust. The location of slab dehydration reactions and zones of high fluid flux depends critically on the subsolidus basaltic phase diagram. Unfortunately, few subsolidus phase equilibria experiments of hydrous basaltic compositions have been performed at pressures greater than 10 kbar. The anhydrous nature of most eclogites suggests that much of the H_2O in subducted oceanic crust is driven off at relatively shallow depths (less than 50 km).

In a previous paper (Peacock 1990*b*), I presented the results of numerical experiments that incorporated several different models of dehydration in subducting oceanic crust. In these calculations the 7.5 km thick oceanic crust was assumed to contain 2 wt% bound H_2O (a probable maximum amount) distributed homogeneously throughout the crust. Fluids were released by continuous and discontinuous end-members of three different dehydration models: pressure-sensitive, temperature-sensitive, and amphibole (negative dP/dT) dehydration. For a convergence rate of 3 cm a^{-1}, typical fluid fluxes out of the subducting slab range from *ca.* 0.1 (kg fluid) m^{-2} a^{-1} for the continuous reaction models to more than 1 (kg fluid) m^{-2} a^{-1} for the discontinuous pressure and amphibole dehydration models. These fluid fluxes should be considered maxima because of the assumption that 2 wt% H_2O is released.

Under a relatively restricted set of conditions, fluids released by slab dehydration reactions could trigger partial melting in overlying oceanic crust (figure 3). During subduction, fluids released from the base of the subducting oceanic crust will travel up temperature if they flow up toward the subduction shear zone. Upward fluid flow will trigger fluid-present partial melting reactions in the subducting slab if the temperature at the top of the subducting oceanic crust exceeds the wet basaltic solidus. This scenario occurs only if P–T–t paths for the top and base of the subducting oceanic crust straddle a temperature-sensitive dehydration reaction and the wet basaltic solidus as depicted by paths C and C′ in figure 3.

More commonly, fluids released by metamorphic reactions in the subducting oceanic crust that travel up the subduction shear zone would not be expected to trigger melting reactions. During subduction, H_2O-rich fluids released by dehydration reactions in the oceanic crust may drive decarbonation reactions in overlying pelagic sediments. Fluids that migrate up the subduction shear zone could cause hydration and carbonation reactions in oceanic crust at shallower levels in the subduction zone, or such fluids could be expelled through the accretionary prism.

In relatively warm subduction zones, formed in young oceanic lithosphere (less than 50 Ma), subducting oceanic crust intersects the wet basaltic solidus at pressures less than 28 kbar. The amount of partial melting that will occur above the wet solidus will be proportional to the amount of free H_2O present in the rock. The porosity of subducted oceanic crust at depths of *ca.* 100 km is unknown, but presumably small. If we assume a porosity of 0.3% filled with pure H_2O (equivalent to 0.1 wt % free H_2O in the rock) and that the melt phase contains 5 wt % H_2O, then approximately 2 % partial melt would form by fluid-present melting at temperatures above the wet solidus. As the oceanic crust is subducted to deeper levels, *P–T–t* paths intersect a major partial melting reaction caused by the breakdown of hornblende; substantial amounts of magma could form by this fluid-absent partial melting reaction in warm subduction zones.

P–T–t paths for relatively cool subduction zones do not intersect the wet basaltic solidus until pressures greater than 50 kbar (figure 3) suggesting that partial melting of subducting oceanic crust is an unlikely magma source in mature subduction zones or subduction zones that form in old oceanic lithosphere. Under such conditions the subducting oceanic crust should dehydrate before encountering any partial melting reactions. If the calculated position of the tremolite dehydration reaction (figure 3) represents a good approximation to the *P–T* location of the amphibole dehydration in metabasalt, then this reaction would generate substantial amounts of H_2O at depths of 100–150 km.

(*b*) *Hydration and partial melting of the mantle wedge*

Studies of ancient and modern subduction zones demonstrate that some of the fluids released from the subducting slab migrate upward into the overlying mantle wedge. Evidence for fluid infiltration of the mantle wedge includes the presence of serpentinite diapirs in the Marianas forearc (Fryer *et al.* 1985) and pervasively hydrated and metasomatized ultramafic hanging walls of the Trinity thrust system (Peacock 1987*a*) and the Catalina Schist terrane (Bebout & Barton 1989).

The consequences of fluid infiltration of the overlying mantle wedge may be investigated by combining mantle wedge *P–T–t* paths with the phase diagram for peridotite bulk compositions (figure 4). The effect of fluid infiltration depends critically on the temperature of the portion of the mantle wedge being infiltrated. If H_2O infiltrates the mantle wedge at temperatures below the ‘hornblende-out’ and ‘phlogopite-out’ partial melting reactions, then infiltrating H_2O will react with peridotite to form phlogopite (plus amphibole at $P < 28$ kbar). The amount of phlogopite ± amphibole that can form from H_2O infiltration depends on the amount of K, Na, Ca, and Al present in the peridotite plus the amount of these elements carried in by the fluid. Once the rocks capacity to form these minerals is exceeded, further H_2O infiltration at temperatures above the wet solidus will cause fluid-present partial melting to occur. Based on the phase diagram presented in figure 4, after phlogopite ± amphibole formation, H_2O should coexist as a free fluid with peridotite at temperatures less than the wet peridotite solidus and greater than *ca.* 700 °C. In this narrow temperature range, H_2O should pass through the mantle wedge without causing hydration or partial melting reactions. The infiltration of H_2O into the mantle wedge at temperatures below *ca.* 700 °C should form additional hydrous phases such as talc and chlorite.

In the absence of induced convection, mantle wedge rocks follow isobaric cooling trajectories (figure 4*a*). In general, fluid infiltration of the mantle wedge could cause partial melting during the early stages of subduction if temperatures exceed the wet peridotite solidus. As subduction progresses and the mantle wedge cools, most fluid infiltration will occur at subsolidus conditions and should cause hydration rather than partial melting.

In the presence of induced convection, rocks in the mantle wedge follow more complex *P–T–t* paths (figure 4*b*, *c*). In subduction zones where induced asthen-

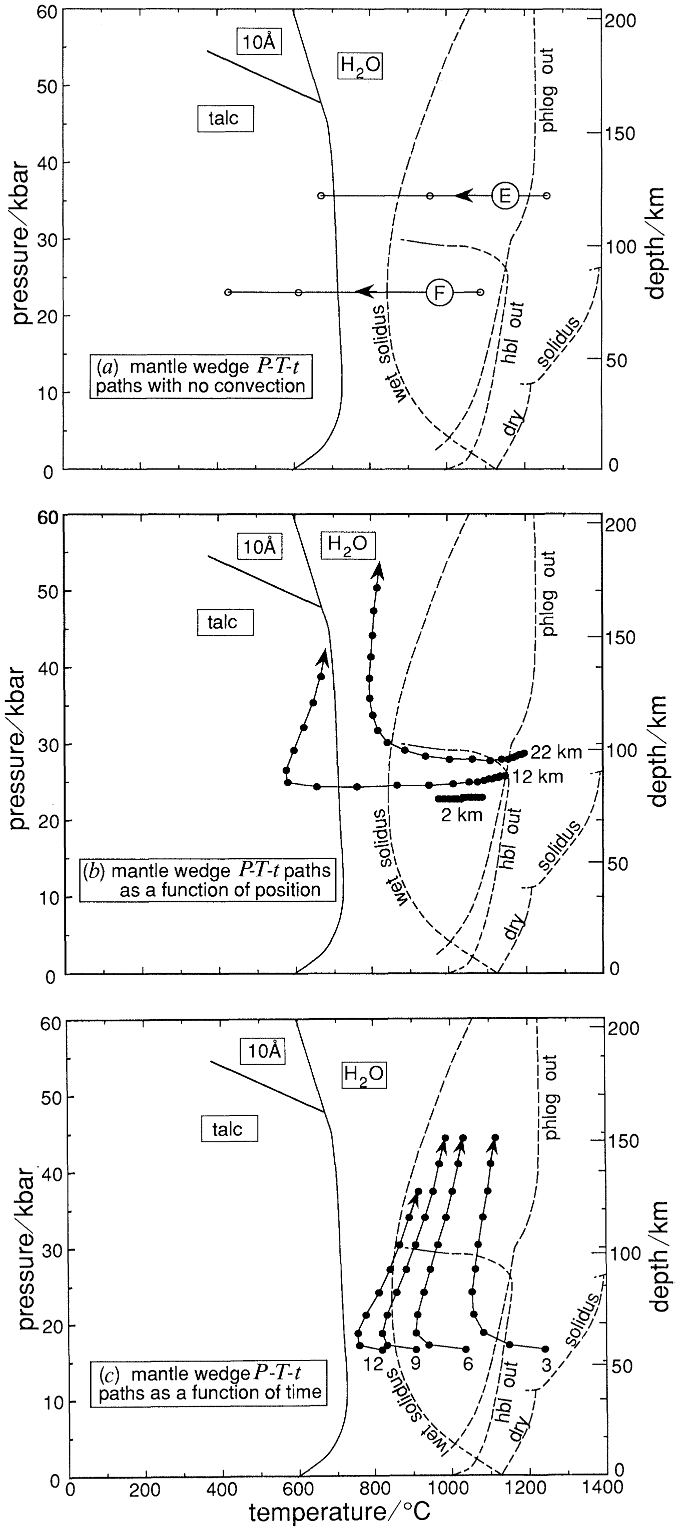

Figure 4. For description see opposite.

ospheric wedge flow occurs at relatively shallow depths (less than 100 km), peridotite containing hornblende formed by H_2O infiltration can be dragged across the 'hornblende-out' partial melting reaction (figure 4*c*). In subduction zones, large amounts of partial melt may be generated by this reaction (Tatsumi 1989).

The pressure-dependent portion of the 'hornblende-out' partial melting reaction in peridotite bulk compositions may be the source of arc magmas in subduction zones that have convecting asthenosphere above the subducting slab at shallow depths (less than 100 km) (figure 4*c*). In the numerical experiments described in this paper, the lithosphere/asthenosphere boundary is fixed by the 1300 °C isotherm in the initial oceanic geotherm. Thus, shallow convecting asthenosphere is only present in the experiments conducted for young (less than 10 Ma) oceanic lithosphere. In experiments simulating subduction zones formed in older oceanic lithosphere, mantle wedge P–T–t paths lie at pressures greater than the 'hornblende-out' partial melting reaction. If lower temperature material convects (e.g. the lithosphere/asthenosphere boundary is fixed at, say, 1100 °C), then the 'hornblende-out' partial melting reaction could be an important source of arc magmas in many subduction zones.

In modern subduction zones, asthenosphere appears to be present beneath most, if not all, magmatic arcs (Gill 1981). For example, beneath the northeast Japan volcanic arc, a low-velocity–low-Q region (asthenosphere) exists directly beneath the 35 km thick crust (Yoshii 1979). Because the Japan subduction zone formed in old (*ca.* 150 Ma) oceanic lithosphere, one might expect the overriding Japan plate to have a thick lithosphere. The apparent absence of lithospheric mantle beneath Japan may be explained by (1) tectonic erosion during subduction initiation; (2) thermal erosion caused by induced asthenospheric flow; or (3) crust/lithosphere decoupling during back-arc extension.

Future numerical experiments will focus on simulating modern subduction zones where the lithospheric structure of the subducting and overriding plates differ, developing more realistic petrogenetic grids, and evaluating different rheological models for the mantle.

Figure 4. Experimental partial-melting (dashed lines) and subsolidus phase relations (solid lines) applicable to the peridotite + H_2O system. As in the basalt system, the presence of excess H_2O decreases the melting temperature of peridotite (dry solidus: Takahashi & Kushiro 1983; wet solidus: Mysen & Boettcher 1975). Amphibole and phlogopite are stable on the solidus up to *ca.* 30 kbar and greater than 50 kbar, respectively. The 'hbl out' and 'phlog out' curves represent fluid-absent partial melting of hornblende-bearing and phlogopite-bearing peridotite, respectively (hbl out: Green 1973; phlog out: Wendlendt & Eggler 1980). Minerals in boxes represent the stable hydrous phase that coexists with forsterite + enstatite in the simplified $MgO–SiO_2–H_2O$ peridotite system (Kitahara *et al.* 1966; Yamamoto & Akimoto 1977). Additional hydrous phases, such as phlogopite and amphibole, will be stable in the more complex peridotite chemical system. Thermodynamic calculations suggest that serpentine may coexist with forsterite and enstatite at temperatures less than 600 °C and pressures greater than *ca.* 20 kbar. Convergence rate is 3 cm a^{-1}. (*a*) In the absence of induced mantle wedge convection (P–T–t paths E and F), the mantle wedge cools isobarically. (*b*) P–T–t paths followed by convecting mantle wedge. Rocks are initially located 2, 12 and 22 km beneath 75 km thick lithosphere, and 150 km from the asthenospheric wedge tip. (*c*) P–T–t paths followed by convecting mantle wedge as a function of time in millions of years. Rocks start near asthenospheric wedge tip and are dragged down with the slab. Initial oceanic geotherm is 10 Ma.

5. Summary

Computer simulation of heat transfer provides a powerful means by which to investigate the location and sequence of metamorphic and igneous reactions that occur at depth in subduction zones. The results of the experiments described above suggest that partial melting of the subducting oceanic crust should only occur during the early stages of subduction initiated in young (less than 50 Ma) oceanic lithosphere. For many subduction zones, partial melting appears to be the result of H_2O infiltration into the convecting mantle wedge. Partial melting of the mantle wedge may occur (1) by H_2O infiltration at temperatures above the wet peridotite solidus after phlogopite ± amphibole formation or (2) by a two-stage process in which amphibole is first formed and subsequently destroyed as the rock is dragged downward across the 'hornblende-out' partial melting reaction.

I thank the organizers of this meeting for inviting me to present the results of my research. I thank Professor Bickle and Professor Barnicoat for their insightful reviews. This research was supported by National Science Foundation grant EAR-87-20343.

References

Anderson, R. N., Uyeda, S. & Miyashiro, A. 1976 Geophysical and geochemical constraints at converging plate boundaries. I. Dehydration in the downgoing slab. *Geophys. Jl R. astr. Soc.* **44**, 333–357.

Anderson, R. N., DeLong, S. E. & Schwarz, W. M. 1978 Thermal model for subduction with dehydration in the downgoing slab. *J. Geol.* **86**, 731–739.

Anderson, R. N., DeLong, S. E. & Schwarz, W. M. 1980 Dehydration, asthenospheric convection and seismicity in subduction zones. *J. Geol.* **88**, 445–451.

Andrews, D. J. & Sleep, N. H. 1974 Numerical modeling of tectonic flow behind island arcs. *Geophys. Jl R. astr. Soc.* **38**, 237–251.

Basaltic Volcanism Study Project 1981 *Basaltic volcanism on the terrestrial planets*. New York: Pergamon Press.

Batchelor, G. K. 1967 *An introduction to fluid dynamics*. Cambridge University Press.

Bebout, G. E. & Barton, M. D. 1989 Fluid flow and metasomatism in a subduction zone hydrothermal system: Catalina Schist terrane, California. *Geology* **17**, 976–980.

Berman, R. G. 1988 Internally-consistent thermodynamic data for minerals in the system. *J. Petrol.* **29**, 445–522.

Delany, J. M. & Helgeson, H. C. 1978 Calculation of the thermodynamic consequences of dehydration in subducting oceanic crust to 100 kb and > 800 °C. *Am. J. Sci.* **278**, 638–686.

Ernst, W. G. 1988 Tectonic history of subduction zones inferred from retrograde blueschist *P–T* paths. *Geology* **16**, 1081–1084.

Evans, B. W. & Brown, E. H. (eds) 1986 *Blueschists and eclogites*. Geol. Soc. Am. Memoir 164.

Fryer, P., Ambos, E. L. & Hussong, D. M. 1985 Origin and emplacement of Mariana forearc seamounts. *Geology* **13**, 774–777.

Green, D. H. 1973 Experimental melting studies on a model upper mantle composition at high pressure under water-saturated and water-undersaturated conditions. *Earth planet. Sci. Lett.* **19**, 37–53.

Green, T. H. 1982 Anatexis of mafic crust and high pressure crystallization of andesite. In *Andesites* (ed. R. S. Thorpe), pp. 465–487. London: Wiley.

Gill, J. 1981 *Orogenic andesites and plate tectonics*. New York: Springer-Verlag.

Hasebe, K., Fujii, N. & Uyeda, S. 1970 Thermal processes under island arcs. *Tectonophys.* **10**, 335–355.

Honda, S. & Uyeda, S. 1983 Thermal processes in subduction zones – a review and preliminary approach on the origin of arc volcanism. In *Arc volcanism: physics and tectonics* (ed. D. Shimozuru & I. Yokoyama), pp. 117–140. Tokyo: Terra Scientific.

Jeanloz, R. & Morris, S. 1986 Temperature distribution in the crust and mantle. *A. Rev. Earth planet. Sci.* **14**, 377–415.

Kitahara, S., Takenouchi, S. & Kennedy, G. C. 1966 Phase relations in the system $MgO–SiO_2–H_2O$ at high temperatures and pressures. *Am. J. Sci.* **264**, 223–233.

Lambert, I. B. & Wyllie, P. J. 1972 Melting of gabbro (quartz eclogite) with excess water to 35 kilobars, with geological applications. *J. Geol.* **80**, 695–708.

Minear, J. W. & Toksoz, N. M. 1970 Thermal regime of a downgoing slab and new global tectonics. *J. geophys. Res.* **75**, 1397–1419.

Mysen, B. O. & Boettcher, A. L. 1975 Melting of a hydrous mantle: I. Phase relations of natural peridotite at high pressures and temperatures with controlled activities of water, carbon dioxide, and hydrogen. *J. Petrol.* **16**, 520–548.

Oxburgh, E. R. & Turcotte, D. L. 1970 Thermal structure of island arcs. *Geol. Soc. Am. Bull.* **81**, 1665–1688.

Oxburgh, E. R. & Turcotte, D. L. 1976 The physico-chemical behavior of the descending lithosphere. *Tectonophys.* **32**, 107–128.

Peacock, S. M. 1987*a* Serpentinization and infiltration metasomatism of the Trinity peridotite, Klamath province, northern California: implications for subduction zones. *Contrib. Mineral. Petrol.* **95**, 55–70.

Peacock, S. M. 1987*b* Creation and preservation of subduction-related inverted metamorphic gradients. *J. geophys. Res.* **92**, 12763–12781.

Peacock, S. M. 1987*c* Thermal effects of metamorphic fluids in subduction zones. *Geology* **15**, 1057–1060.

Peacock, S. M. 1990*a* Fluid processes in subduction zones. *Science, Wash.* **248**, 329–337.

Peacock, S. M. 1990*b* Numerical simulation of metamorphic pressure–temperature–time paths and fluid production in subducting slabs. *Tectonics* **9**, 1197–1211.

Platt, J. P. 1975 Metamorphic and deformational processes in the Franciscan Complex, California: Some insights from the Catalina Schist terrane. *Geol. Soc. Am. Bull.* **86**, 1337–1347.

Sorensen, S. S. 1986 Petrologic and geochemical comparison of the blueschist and greenschist units of the Catalina Schist terrane, southern California. *Geol. Soc. Am. Mem.* **164**, 59–75.

Sorensen, S. S. 1988 Petrology of amphibolite-facies mafic and ultramafic rocks from the Catalina Schist, southern California: metasomatism and migmatization in a subduction zone metamorphic setting. *J. metam. Geol.* **6**, 405–435.

Stacey, F. D. 1977 *Physics of the Earth*, 2nd edn. New York: Wiley.

Takahashi, E. & Kushiro, I. 1983 Melting of a dry peridotite at high pressures and basalt magma genesis. *Am. Mineral.* **68**, 859.

Tatsumi, Y. 1989 Migration of fluid phases and genesis of basalt magmas in subduction zones. *J. geophys. Res.* **94**, 4697–4707.

Toksoz, M. N., Minear, J. W. & Julian, B. R. 1971 Temperature field and geophysical effects of a downgoing slab. *J. geophys. Res.* **76**, 1113–1138.

van der Beukel, J. & Wortel, R. 1986 Thermal modelling of arc-trench regions. *Geol. Mijnbouw* **65**, 133–143.

Wendlandt, R. F. & Eggler, D. H. 1980 The origins of potassic magmas: 1. Melting relations in the systems $KAlSiO_4–Mg_2SiO_4–SiO_2$ and $KAlSiO_4–MgO–SiO_2–CO_2$ to 30 kilobars. *Am. J. Sci.* **280**, 385–420.

Wyllie, P. J. 1988 Magma genesis, plate tectonics, and chemical differentiation of the earth. *Rev. Geophys.* **26**, 370–404.

Wyllie, P. J. & Sekine, T. 1982 The formation of mantle phlogopite in subduction zone hybridization. *Contrib. Mineral. Petrol.* **79**, 375–380.

Yamamoto, K. & Akimoto, S. I. 1977 The system $MgO–SiO_2–H_2O$ at high pressures and temperatures – stability field for hydroxyl – chondrodite, hydroxyl – clinohumite and 10 Å-phase. *Am. J. Sci.* **277**, 288–312.

Yoshii, T. 1979 A detailed cross-section of the deep seismic zone beneath northeastern Honshu, Japan. *Tectonophys.* **55**, 349–360.